ANTIOXIDANTS & REDOX SIGNALING
Volume 14, Number 6, 2011

DOI: 10.1089/ars.2010.3444

ORIGINAL RESEARCH COMMUNICATION

The p53/p21$^{WAF/CIP}$ Pathway Mediates Oxidative Stress and Senescence in Dyskeratosis Congenita Cells with Telomerase Insufficiency

Erik R. Westin,[1] Nukhet Aykin-Burns,[2] Erin M. Buckingham,[3] Douglas R. Spitz,[2] Frederick D. Goldman,[4] and Aloysius J. Klingelhutz[1–3]

Abstract

Telomere attrition is a natural process that occurs due to inadequate telomere maintenance. Once at a critically short threshold, telomeres signal growth arrest, leading to senescence. Telomeres can be elongated by the enzyme telomerase, which adds *de novo* telomere repeats to the ends of chromosomes. Mutations in genes for telomere binding proteins or components of telomerase give rise to the premature aging disorder dyskeratosis congenita (DC), which is characterized by extremely short telomeres and an aging phenotype. The current study demonstrates that DC cells signal a DNA damage response through p53 and its downstream mediator, p21$^{WAF/CIP}$, which is accompanied by an elevation in steady-state levels of superoxide and percent glutathione disulfide, both indicators of oxidative stress. Poor proliferation of DC cells can be partially overcome by reducing O_2 tension from 21% to 4%. Further, restoring telomerase activity or inhibiting p53 or p21$^{WAF/CIP}$ significantly mitigated growth inhibition as well as caused a significant decrease in steady-state levels of superoxide. Our results support a model in which telomerase insufficiency in DC leads to p21$^{WAF/CIP}$ signaling, *via* p53, to cause increased steady-state levels of superoxide, metabolic oxidative stress, and senescence. *Antioxid. Redox Signal.* 14, 985–997.

Introduction

Cellular aging involves the interaction between biological programming and numerous environmental factors that culminate in cells losing the ability to proliferate and becoming senescent. Two well-characterized intracellular mechanisms that are believed to induce senescence are telomere shortening and oxidative stress, both of which are thought to be causative factors in aging (4, 17).

Reactive oxygen species (ROS) are a diverse set of reactive molecules such as hydrogen peroxide, organic hydroperoxides, superoxide ($O_2^{\bullet -}$), and hydroxyl radicals ($^{\bullet}OH$) that, in excess, can cause oxidative stress and facilitate entry into senescence (17). ROS have been found to be elevated in aged tissues and can be manipulated *in vitro* to induce senescence (39). In agreement with the idea that reactions involving oxygen (O_2) can contribute to senescence, early studies indicated that increasing ambient O_2 tension in cell culture environments hastened entry into senescence, whereas decreasing the O_2 tension from 21% to ~4% increased replicative lifespan (17). To mitigate the potential toxicity associated with elevated ROS, cells express several redundant antioxidant enzyme systems, including superoxide dismutases (SOD) [Cu(Zn)SOD, MnSOD, and extracellular SOD], catalase, peroxiredoxins, and glutathione (GSH) peroxidases. When steady-state levels of ROS exceed antioxidant capacity, oxidative stress ensues, which can contribute to cell death or entry into senescence. Phylogenetic studies investigating the role of oxidative stress in aging have found that ROS production or detoxification are strong determinates of organismal lifespan (34). Interestingly, *in vitro* evidence indicates that the DNA damage response can cause an increase in ROS and that the irreversible nature of senescence is dependent on ROS (47).

Telomere shortening is believed to act as a mitotic clock to limit replicative lifespan (4). Telomeres are a highly conserved evolutionary mechanism utilized across many species to cap the ends of linear chromosomes. In humans, telomeres are composed of tandem arrays of the hexameric DNA repeat, TTAGGG. Telomeres shorten with each successive cell division unless maintained by telomerase, a ribonucleoprotein

[1]Interdisciplinary Program in Genetics, [2]Free Radical and Radiation Biology Program, Department of Radiation Oncology, Holden Comprehensive Cancer Center, and [3]Department of Microbiology, University of Iowa, Iowa City, Iowa.
[4]Department of Pediatrics, University of Alabama, Birmingham, Alabama.

reverse transcriptase capable of adding *de novo* repeats to chromosomal termini (12). One factor that results in telomere diminution is the end-replication problem, whereby DNA replication fails to faithfully replicate chromosome ends leading to continuous attrition (23). Interestingly, it has also been demonstrated that ROS can accelerate telomere shortening (48). Aside from protecting genes within the chromosome from undergoing erosion, it is also thought that telomeres provide the framework for a protein-containing secondary structure called a telomere-loop, which prevents the cell machinery from recognizing the telomere as a double-stranded DNA break (20). Once critically shortened, the telomere structure is disrupted, initiating a pathway that activates a DNA damage response (DDR) (14). This telomere-associated DDR involves, in part, a sequence of events that lead to deposition of DDR marks such as p53 binding protein 1 (53BP1) and γ-H2AX within the telomere, which lead the subsequent activation of the kinases ATM/ATR, CHK1/CHK2, the tumor suppressor p53, and the p53-regulated cyclin-dependent kinase inhibitor (CDKi), $p21^{WAF/CIP}$. Evidence has also been found supporting a role for another CDKi and associated protein, the protein 16 inhibitor of kinase 4a ($p16^{INK4A}$)-RB pathway, in mediating telomere-associated cellular senescence (26).

In a small fraction of cells (*i.e.*, embryonic, germ, and hematopoietic stem cells as well as activated T-cells) telomere maintenance is performed by a complex of proteins that together constitute the enzymatic activity of telomerase (13). Telomerase is minimally comprised of a reverse transcriptase catalytic moiety (telomerase reverse transcriptase [TERT]) and its RNA template strand (telomerase RNA component [TERC]). Telomere extension by telomerase can extend the proliferative capacity of some cells that would otherwise be susceptible to replicative senescence (7). However, aberrant telomerase activity has potentially grave consequences as it has been found to be activated in $\sim$90% of tumors/cancers (30).

A human disease caused by inadequate telomere maintenance, dyskeratosis congenita (DC), is primarily a bone marrow failure disorder but also displays a wide variety of other aging phenotypes that make DC a highly relevant model for understanding the relationship between telomeres and human aging (32). Clinical features of DC patients include a rare triad of nail dystrophy, skin pigmentation, and oral leukoplakia in addition to premature alopecia, graying of hair, and osteoporosis. These symptoms, coupled with a high incidence of bone marrow failure, liver dysfunction, pulmonary fibrosis, and malignancy suggest that certain tissues may be more susceptible to telomere dysfunction *in vivo*. Mutations in at least five telomerase or telomere-related genes have been found to cause DC (32). The first reported mutation to cause autosomal dominant DC (ADDC) was described in a three-generation family harboring a mutation in the 3′ terminus of the *TERC* gene (49). In this family, the disease is caused by haploinsufficiency where affected individuals have one wild-type and one mutant copy of *TERC*. Mutations in *TERT* and *TERC* have also been reported in patients with pulmonary fibrosis and aplastic anemia (and other bone marrow failure syndromes) without clinical manifestations common to DC, indicating that insufficient telomerase and critically short telomeres may play a key role in the pathogenesis of non-DC diseases that display symptoms related to DC patients (4).

Previous work by our lab identified short telomeres, decreased proliferative capacity, increased population doubling time, and a prematurely senescent phenotype in cells from DC donors that were ameliorated by exogenous expression of telomerase components (19, 33, 50). In the current study, we have uncovered evidence of increased steady-state levels of superoxide and oxidative stress in DC cells that is mediated by the $p53/p21^{WAF/CIP}$ pathway. In addition, the proliferative defect in DC cells is O_2 dependent and can be corrected by introduction of exogenous telomerase as well as partially ameliorated by inhibition of p53 or $p21^{WAF/CIP}$, which also reduces steady-state levels of superoxide. These studies demonstrate a link between a relevant human disease caused by telomerase/telomere dysfunction and increased steady-state levels of superoxide that is mediated by the $p53/p21^{WAF/CIP}$ pathway. Our results suggest new mechanistic insights that could be exploited to provide some relief from the symptoms of this disease.

Materials and Methods

Cells

Cells from DC subjects and healthy controls were obtained with consent and approval from the University of Iowa Internal Review board. These patients are part of a multigenerational kindred with a deletion that encompasses the terminal 74 base pairs of the processed/expressed *TERC* gene giving rise to a haploinsufficient, autosomal dominant form of DC (49). Skin fibroblasts were acquired *via* punch biopsies and were grown in Dulbecco's modified Eagle's medium supplemented with 10% fetal bovine serum as previously published (50). Experiments to compare DC and normal cells were always carried out at similar passage number. Lymphocytes were isolated following Ficoll-Hypaque (GE Healthcare) gradient separation of whole blood obtained following venipuncture and grown in RPMI media and 10% fetal calf serum with antibiotics as previously described (33). $CD3^+$ lymphocytes were isolated by positive selection using recommended protocols (Stem Cell Technology). Keratinocytes were isolated and cultured as previously described (19). All experiments were performed using DC and normal fibroblasts at the same passage unless indicated otherwise.

Growth kinetics

DC and control skin fibroblasts were plated at 15,000 cells per 60 mm tissue culture plate in triplicate sets. Cells were in media conditions previously mentioned under either ambient O_2 (21%) or reduced O_2 (4%). Cells were passaged at 50%–70% confluency to maintain log phase growth. At intermittent periods, triplicate sets were washed, trypsinized, and counted using a Coulter Counter. Error bars represent the standard deviation of the triplicate sets.

Senescence-associated β-galactosidase assay

The senescence-associated β-galactosidase assay was performed using a previously published protocol (16). Briefly, DC and normal cells at the same passage were grown subconfluently in Dulbecco's modified Eagle's medium/10% fetal bovine serum in six-well plates, the cells were fixed, and staining solution was left overnight. Low-power photos of images containing >200 cells were taken using bright-field

microscope, and total and blue-colored cells were counted. Error bars indicate the standard deviation among triplicate wells analyzed.

Retroviral constructs and transduction of cells

The mutant mito-TERT R3E/R6E construct was generated by removing the mitochondrial localization signal of TERT (43) by site-directed mutagenesis (QuikChange; Stratagene) and inserting this into pLXSN. LXSN-TERT and feline immunodeficiency virus-U3-hTERC have been published elsewhere (50). Other constructs were obtained from various sources, including sh-p53 pBABE-hygro (Dr. Carla Grandori), sh-p21-GIPZ (Dr. Toru Nyunoya), sh-p16 MSCV (Dr. Scott Lowe), dominant-negative TERT-pBABE-neo (Dr. Bill Hahn), TERT-dissociation of activities of telomerase (DAT) mutants (N-DAT +92, +122, +128) in pBABE-neo (Dr. Christopher Counter), DN-telomere repeat binding factor 2 (TRF2)-pBABE-Puro (Dr. Titia de Lange), and TERT-pBABE-neo (Dr. Robert Weinberg). To produce virus carrying the genes of interest, retroviral plasmids were incubated with GenePORTER (Genlantis) according to the manufacture's protocol. This cocktail was then added to amphotropic-expressing Phoenix cells and supernatants were prepared as previously published (15). Fibroblast infections took place in the presence of 8 μg/ml polybrene overnight. Cells were selected with a respective antibiotic (puromycin [1 μg/ml], neomycin [1 mg/ml], or hygromycin [200 μg/ml]). All cells were analyzed before senescence or crisis.

Immunofluorescence

Skin fibroblasts were grown under normal conditions and treated as previously published (24). Briefly, cells were fixed in 4% paraformaldehyde, permeabilized with 0.2% Triton X-100 in phosphate-buffered saline, and subsequently blocked in serum. The 53BP1 antibody (Novus) was diluted 1:500 and incubated overnight. The cells were washed in Tris-buffered saline-Tween20, incubated with secondary antibody, washed, and stained with ToPro-3 (Invitrogen). Cells were observed with a Zeiss 510 multiphoton confocal microscope, captured, and randomized for blinded analysis. Statistical analysis was applied using Student's *t*-test.

Dihydroethidium, glutathione disulfide/GSH, and MitoSOX

Dihydroethidium (DHE; Molecular Probes, Eugene OR) oxidation assays were performed as previously described (46). DHE is oxidized to 2-OH-ethidium in the presence of superoxide and fluoresces. Briefly, triplicate samples of skin fibroblasts, keratinocytes, or T-cells were analyzed during log phase growth and incubated in 10 μM DHE for 40 min. The cells were washed, trypsinized, and centrifugated. The cells were brought up in phosphate-buffered saline and subjected to FACS analysis to quantify relative DHE oxidation levels by comparing the mean fluorescent intensity averages of the triplicate sets. Assays of MitoSOX (Molecular Probes) oxidation were performed similarly, and incubated for a total of 20 min and at a 2 μM concentration. MitoSOX is a mitochondrially targeted DHE that was developed by linking DHE to a triphenylphosphonium cation that is targeted to the mitochondria. It measures superoxide in the mitochondria. Antimycin A (Sigma; 10 μM) was used as a positive control to stimulate DHE and MitoSOX oxidation. Graphs include error bars that represent triplicate sets.

For inhibition of DHE oxidation experiments using polyethylene glycol (PEG)-SOD and PEG-CAT (Sigma) cells were incubated with 100 U/ml PEG-SOD or pegylated-catalase (PEG-CAT) for 1 h and then labeled with 10 μM DHE and incubated for another 40 min following the standard DHE-FACS protocol. The amount of SOD inhibitable (or catalase inhibitable) DHE oxidation was calculated based on the equation: $DHE_{Control} - DHE_{PEG\text{-}SOD}$ = the amount of the mean fluorescent intensity attributable to $O_2^{\bullet -}$; $DHE_{Control} - DHE_{PEG\text{-}CAT}$ = the amount of the mean fluorescent intensity attributable to H_2O_2.

GSH analysis

GSH levels were measured as described previously (45). Briefly, fibroblasts were scraped harvested, spun down, and homogenized in 50 mmol/L potassium phosphate buffer (pH 7.8) containing 1.34 mmol/L diethylenetriaminepentaacetic acid buffer. Total GSH was determined as described (2). GSH and glutathione disulfide were distinguished by addition of 2 μl of a 1:1 mixture of 2-vinylpyridine and ethanol per 30 μl of sample followed by incubation for 1 h before assay (21). Levels of GSH were normalized to cellular protein levels.

Quantitative real-time polymerase chain reaction

Quantitative reverse transcriptase–polymerase chain reaction (QRT-PCR) was utilized to verify diminution of transcript levels when utilizing RNAi technology or for elevated levels of $p16^{INK4A}$. Real-time PCR primers were generated using transcript sequences acquired from NCBI or the UCSC genome browser and analyzed using IDTDNA PrimerQuest analysis. Primer sequences are available upon request. RNA was acquired from fibroblasts by scraping skin fibroblast cultures with 1 ml of TRIzol (Invitrogen). RNA was extracted using RNeasy technology (Qiagen) and utilized for cDNA synthesis (RetroScript, Ambion). The QRT-PCR reaction consisted of synthesized cDNA, oligonucleotide primers (Integrated DNA Technologies), and 2×SYBR-green master-mix (Applied Biosystems) and was run on an ABI PRISM Sequence Detection System (model 7900HT or 7700). The equation $2^{-(\Delta Ct - \Delta RPLP0)}$ was utilized to quantify overall transcript changes between the cell types and normalized to a single gene control, *RPLP0*.

Western blotting

Standard Western blotting techniques were utilized as previously described (15). Briefly, whole cell extracts were acquired from cell scrapings containing WE16 lysis buffer supplemented with protease and phosphatase inhibitors. Protein were separated by sodium dodecyl sulfate–polyacrylamide gel electrophoresis, transferred to a polyvinylidene fluoride membrane, and stained with the following antibodies: $p21^{CDKN1A}$ (Pharminogen) or Actin (Santa Cruz). Secondary antibodies conjugated with HRP were used to illuminate blots with Western Lightning Chemiluminescence Reagent (Perkin-Elmer) and observed on a Fugi LAS 3000 chemiluminescent imager.

Telomerase assay

A quantitative telomerase assay was performed as previously described (19) using 5000 cell equivalents per reaction in quadruplicate.

Statistical analyses

Student's *t*-test was applied where indicated to compare data between samples to assess statistical significance. Error bars within graphs are representative of the standard deviation of replicate samples.

Results

DNA damage response in DC fibroblasts

We have previously reported proliferative defects caused by short telomeres in ADDC cells (19, 33, 50). In addition to this defect, ADDC fibroblasts also exhibited a senescent morphology and an increase in the percentage of cells positively stained for the senescence-associated β-galactosidase (β-gal) marker in comparison to control cells at the same passage (Fig. 1A and Supplementary Fig. S1; Supplementary Data are available online at www.liebertonline.com/ars). In light of this increased β-gal, DC cells were also investigated for the presence of a heightened DDR. In regard to a telomere-DDR, 53BP1 is trafficked relatively early to short or dysfunctional telomeres and serves as a surrogate for the steady-state levels of DDR within a population of cells. Immunofluorescence was employed to enumerate the number of 53BP1 foci per nuclei to ascertain whether DC cells harbor a heightened number of DDR foci. We examined 53BP1 in five different DC samples (DC1-5) obtained from five DC patients and compared to normal control cells at the same passage. All of the DC fibroblasts had a higher number of 53BP1 foci (Table 1). The majority of signals within control normal cells were in the lowest range (0–4 foci), whereas DC cells had more foci per nuclei in the higher bin ranges (5–9 foci and 10–14 foci). An example graph comparing DC-1 to normal cells at the same passage is shown in Figure 1B and a representative immunofluorescence image is shown in Supplementary Figure S2. Thus, DC cells have a significant increase in 53BP1 foci, which is indicative of a heightened DDR.

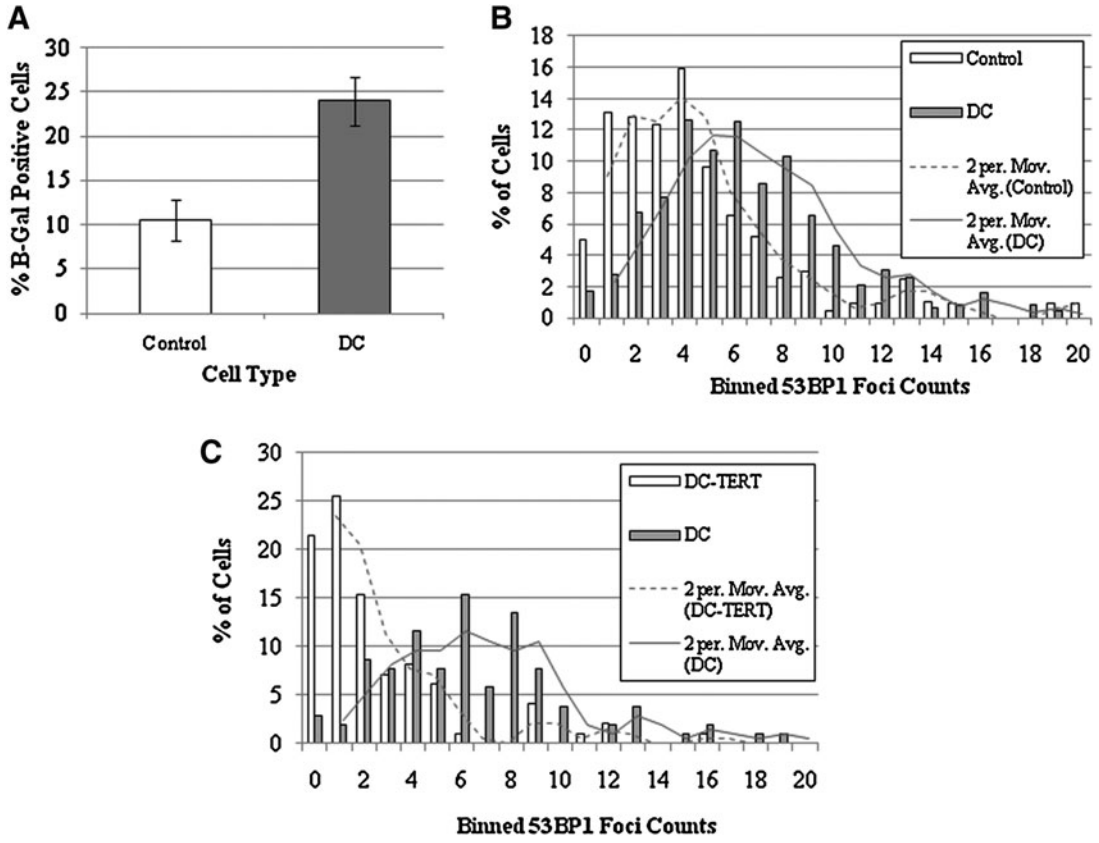

FIG. 1. Heightened telomere DNA damage response in dyskeratosis congenita (DC) cells is mitigated by telomerase activation. (A) DC-1 and normal control cells at the same passage (P7) were assessed for senescence associated β-galactosidase activity as described in the Materials and Methods section. **(B)** DC-1 and normal control cells at the same passage (P8) were assessed for p53 binding protein 1 (53BP1) foci, a marker of DNA damage, as described in the Materials and Methods section. In a blinded fashion, images of 53BP1 focal points were quantified and binned based on counts-per-nucleus. The Y-axis represents the average number of signals per cell acquired per 100 cells (percentage) over two separate experiments. A moving average was calculated to highlight the dissimilarity between the two data sets. The data were subjected to the Student's *t*-test (one-tailed, unequal variance; $p < 0.001$). **(C)** DC-1 cells stably infected with a retrovirus expressing telomerase reverse transcriptase (TERT) were analyzed for changes in 53BP1 foci compared to untransduced DC-1 cells. These data were subjected to the Student's *t*-test (one-tailed, unequal variance; $p < 0.001$).

Table 1. p53 Binding Protein 1 Foci and Phospho-p53 Immunofluorescence in Dyskeratosis Congenita and Normal Cells

Measurement[a]	*Cell type*	*Average*[b]	*Standard error*	*t-Test* (vs. *control*) (p-*value*)
53BP1 foci (per nuclei)	DC1	7.5	0.42	<0.0001
	DC2	6.7	0.50	<0.0001
	DC3	7.3	0.62	<0.0001
	DC4	6.3	0.49	<0.001
	DC5	7.4	0.47	<0.0001
	Control	4.0	0.35	—
p53 Ser15 Signal Intensity (arbitrary units)	DC1	161.0	4.09	<0.0001
	DC2	166.5	5.18	<0.0001
	DC3	149.8	3.97	<0.0001
	DC4	141.3	3.42	<0.0001
	DC5	160.0	2.64	<0.0001
	Control	114.5	3.14	—

[a]53BP1 foci and levels of phospho-serine-15 p53 were assessed as described in the Materials and Methods section.
[b]Average of over 100 nuclei.
53BP1, p53 binding protein 1; DC, dyskeratosis congenita.

In skin fibroblasts, the telomerase activity is restricted by low or absent TERT expression (7). We have shown previously that exogenous expression of TERT in ADDC cells is sufficient to activate telomerase and maintain telomeres, although at a short length (50). Compared to vector control cells, TERT expressing DC-1 and normal cells had much higher telomerase activity (Supplementary Fig. S3). TERT DC-1 cells displayed a dramatic decrease in 53BP1 foci ($p < 0.001$; Fig. 1C). No decrease in 53BP1 foci was observed in TERT expressing normal cells as compared to vector control cells (data not shown). This result suggests that that the higher number of 53BP1 foci in DC cells is due to telomere dysfunction.

Given the heightened number of 53BP1 foci in DC cells, we wanted to determine whether the p53 pathway was activated in these cells. For this purpose, we used immunofluorescence to examine levels of phosphorylation at the serine-15 residue of p53, which is known to occur in the presence of DNA damage (44). Levels of phosphorylated serine-15 were found to be significantly increased in all DC fibroblast strains compared to normal controls at the same passage (Table 1). A graph showing the distribution of the increased signal in DC-1 compared to normal fibroblasts is shown in Figure 2A and a representative immunofluorescence image is shown in Supplementary Figure S2B. Total p53 levels were not increased as measured by immunofluorescence (Supplementary Fig. S4) or Western analysis (data not shown). Upon activation, p53 can transcriptionally upregulate a number of genes, including $p21^{WAF/CIP}$, which was slightly elevated in DC-1 cells as

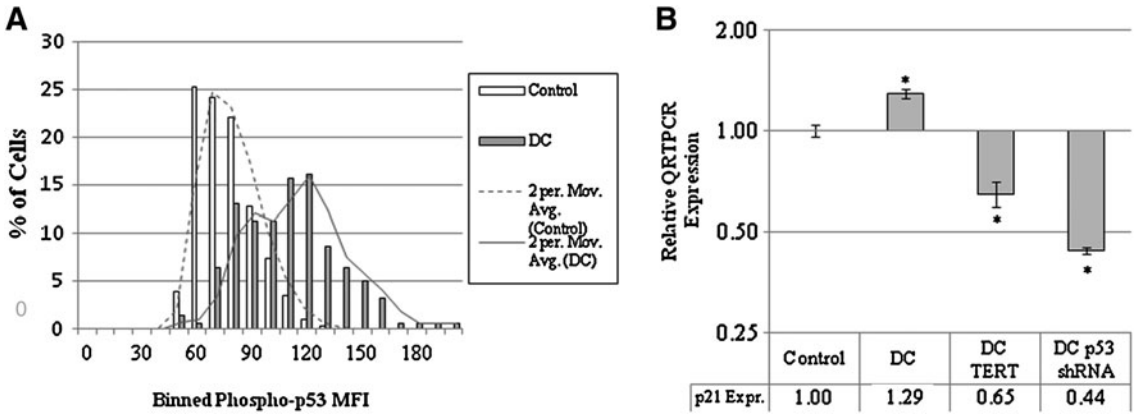

FIG. 2. Activation of the p53/$p21^{WAF/CIP}$ pathway in DC cells. (A) DC-1 and normal control cells at passage 8 were grown under routine conditions, fixed, and stained with a phospho-specific antibody to p53 serine 15, a residue phosphorylated during DNA damage. Images were captured using Zeiss 510 multiphoton confocal microscope and the intensity of nuclear signals was quantified using ImageJ and binned. *p*-Values were generated based on Student's *t*-test ($p < 0.001$). In the inset, representative images are shown. **(B)** RNA was obtained from control cells, DC cells, DC cells expressing exogenous TERT, or p53 short-hairpin RNA (shRNA) grown under routine conditions. cDNA was generated from this RNA to evaluate the relative amount of $p21^{WAF/CIP}$ expressed in these cells. Values were generated based on triplicate quantitative reverse transcriptase–polymerase chain reaction (QRT-PCR) values and graphed (log_2), and data analyzed for statistical significance. Error bars represent standard deviation of triplicates. Student's *t*-test comparisons of DC-1 *versus* Control (normal cells at the same passage), DC-1-TERT *versus* DC-1, and DC-1 p53 shRNA all indicated statistical significance (*$p < 0.001$).

compared to control cells (Fig. 2B). Downregulation of p53 by a short-hairpin RNA (shRNA) (Supplementary Fig. S5A) decreased $p21^{WAF/CIP}$ levels, as did exogenous expression of TERT (Fig. 2B), supporting the hypothesis that short telomeres in DC cells upregulated $p21^{WAF/CIP}$ *via* p53. TERT expression also reduced levels of phospho-p53 in DC cells (data not shown). We also observed an increase in $p16^{INK4A}$ levels in DC cells as compared to controls; however, this increase was not attenuated by TERT expression (data not shown). This indicates that $p16^{INK4A}$ levels were sustained *via* a telomerase-independent mechanism (data not shown). Overall, our data support the existence of a heightened $p53/p21^{WAF/CIP}$ mediated DDR in ADDC fibroblasts that can be repressed upon telomerase activation.

Evidence for oxidative stress in DC cells

Previous studies have indicated that activation of the p53 pathway is associated with an increase in ROS levels (27). To investigate whether the p53 pathway found to be active in DC cells altered intracellular redox state, DC and control fibroblasts at the same passage were analyzed for their ability to oxidize DHE, which is believed to be a surrogate marker for steady-state intracellular superoxide levels (5). Initial experiments using fluorescent microscopy indicated that ADDC fibroblasts exhibit increased DHE oxidation compared to controls (Fig. 3A). To quantify this difference, cells acquired from five ADDC patients and two controls at the same passage were incubated with DHE and analyzed by FACS (fluorescence-activated cell sorting). All five ADDC skin fibroblast samples displayed a statistically significant increase in DHE oxidation compared to controls (Fig. 3B).

Univalent reduction of O_2 to form superoxide is believed to occur during normal O_2 metabolism with $\sim$1% of total O_2 consumption resulting in the formation of superoxide (9), which has been suggested to contribute to the aging process (18). Of importance, pegylated-CuZnSOD (PEG-conjugated CuZnSOD; PEG-SOD) and PEG-CAT are cell-permeable scavengers of superoxide and hydrogen peroxide, respectively, which can be used to determine the involvement of superoxide and hydrogen peroxide in oxidation of fluorescent probes (5). When DC cells were supplemented with PEG-SOD or PEG-CAT and subjected to DHE-FACS analysis, the PEG-SOD inhibitable DHE oxidation (but not PEG-CAT) was significantly elevated in DC cells, clearly demonstrating that the increase in DHE oxidation seen in DC cells was attributable to increased steady-state levels of superoxide in DC cells relative to control (Fig. 3C). To determine if the origin of superoxide production could be localized to mitochondria, MitoSOX oxidation (believed to be targeted to mitochondria) was compared between DC and control cells. As described in the Materials and Methods section, MitoSOX is a mitochondrially targeted DHE. In support of the hypothesis that mitochondria significantly contributed to superoxide levels in DC cells, all five sets of skin fibroblasts acquired from DC patients showed a significant increase in MitoSOX oxidation relative to control (Fig. 3D). The levels of mitochondrial DHE did not strictly correlate with levels of total DHE (compare Fig. 3B and D). Further evidence that DC fibroblasts have increased levels of oxidative stress as compared to normal cells was demonstrated by the observation that DC cells had significantly higher percentages of glutathione disulfide (a major intracellular redox buffer) relative to normal cells at the same passage (Supplementary Fig. S6). To extend these observations to other cell types from DC patients, DHE oxidation was measured in subset of available freshly isolated T-cells and skin keratinocytes from DC patients. Consistent with the findings in fibroblasts, DHE oxidation in this subset of samples was found to be significantly elevated (Fig. 3E, F) relative to age- or passage-matched controls, supporting the hypothesis that several different cell types from DC patients demonstrate increases in steady-state levels of intracellular superoxide. Overall, these results support the hypothesis that insufficient telomerase and the short telomeres observed in cells from DC patients are accompanied by increased steady-state levels of intracellular superoxide.

Expression of TERT in DC cells decreases steady-state levels of superoxide

To determine if there was a causal relationship between diminished telomerase function and alterations in steady-state levels of superoxide, the effects of TERT expression on steady-state levels of DHE oxidation was determined in DC cells. DC and control cells were infected with vector alone or the same vector containing TERT, which mobilizes telomerase activity in skin fibroblasts (Supplementary Fig. S3). TERT-expressing DC cells exhibited a significant 50% decrease in both DHE and MitoSOX oxidation, relative to empty vector treated cells (Fig. 4A, B), demonstrating that overexpression of TERT in DC cells decreased steady-state levels of superoxide. These data, along with our previous work showing maintenance of telomeres and amelioration of proliferative defects in DC cells by expression of TERT (50), indicate that the higher steady-state levels of superoxide in DC cells are linked to telomerase insufficiency and shortened telomeres.

Although the primary function of telomerase is to maintain and elongate telomeres, recent reports have uncovered extra-telomeric secondary functions of TERT (8). To determine whether any of these other functions accounted for the effects of TERT expression on superoxide levels in DC cells, TERT variants with targeted mutations in key domains were exploited. These TERT modifications include mutations that (i) disrupt the ability of TERT to be trafficked to the mitochondria (*i.e.*, R3E/R6E) (43), (ii) mutations that disrupt telomere elongation (3) but retain the ability to assist in a putative DNA damage function (*i.e.*, TERT-DAT mutants) (37), and (iii) a dominant negative TERT unable to elongate telomeres (*i.e.*, DN-TERT) (22). The DN-TERT and TERT-DAT mutants failed to decrease DHE, whereas the R3E/R6E TERT mutant decreased ROS comparable to wild-type TERT (Fig. 4C). These results indicate that the putative mitochondrial targeting signal and the DNA damage-related function of TERT are dispensable for decreasing steady-state levels of superoxide in DC cells, suggesting that the telomere maintenance function of TERT is critical to the decreased superoxide levels demonstrated by DC cells expressing TERT. Overall, these results show that the telomere-elongating function of TERT must remain intact to reduce steady-state levels of superoxide in DC cells.

To further test the hypothesis that short telomeres lead to increased steady-state levels of superoxide, a dominant-negative version of a telomere binding protein, TRF2 (DN-TRF2),

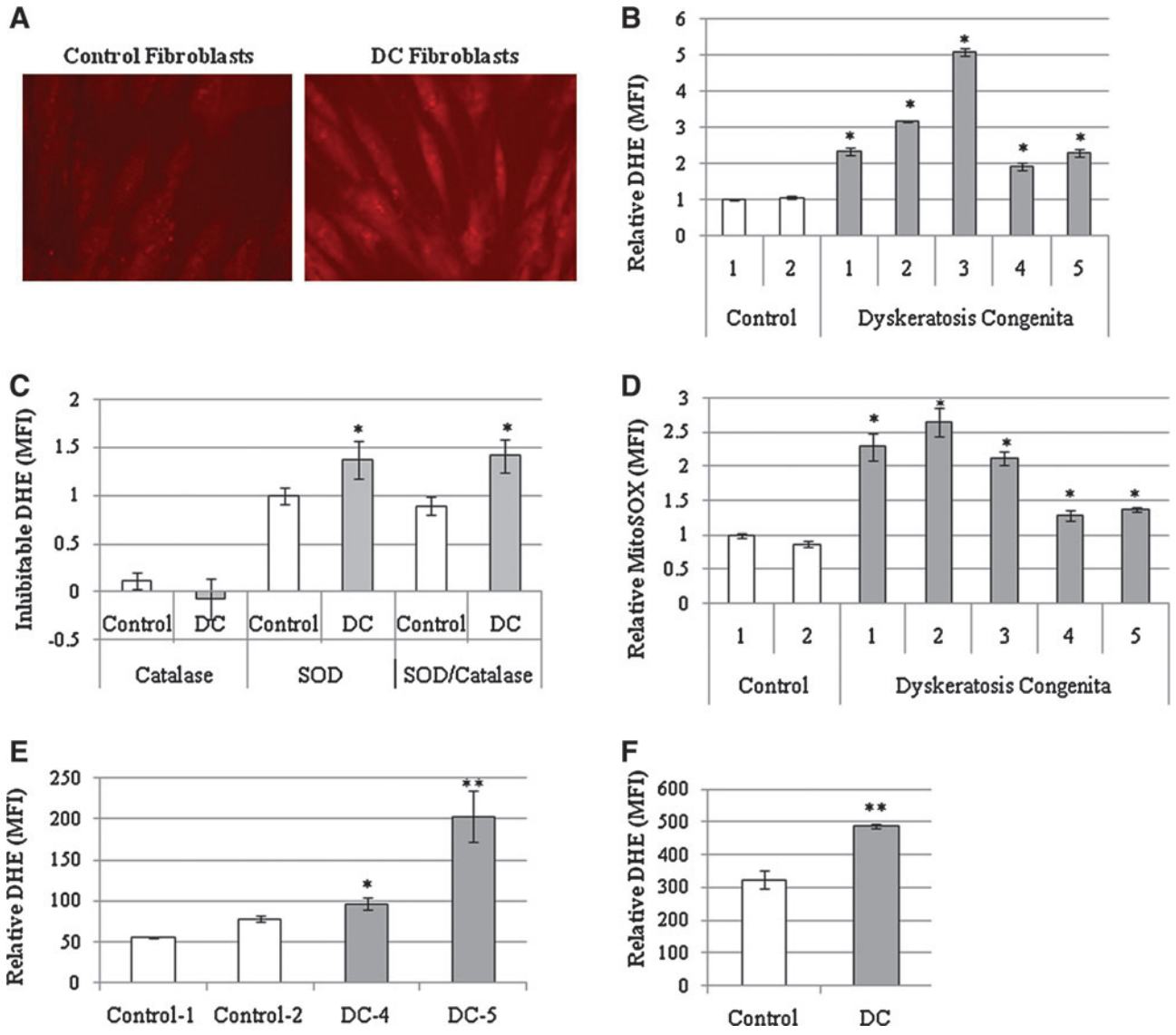

FIG. 3. Measurement of elevated steady-state levels of superoxide in DC fibroblasts. Qualitative assessment of control **(A)** and DC-1 and normal fibroblasts at the same passage (P8) were incubated with dihydroethidium (DHE) and observed with a Zeiss 510 multiphoton confocal microscope. **(B)** Samples from two normal controls and five DC family members (DC1–5) were quantified for DHE oxidation using FACS analysis. DHE oxidation values represent the mean fluorescent intensity (MFI) from the measurement of 10,000 cells. The error bars are reflective of standard deviation in triplicate analyses of cells from each individual. Data are normalized to the MFI value from control fibroblasts. *Statistically significant increase in DHE oxidation compared to controls, $p < 0.001$. **(C)** DC-1 and normal control fibroblasts at P8 were labeled under routine conditions in the presence of DHE or DHE + pegylated SOD and/or catalase. The values represent the difference between cells incubated in DHE (total DHE oxidation) and cells incubated with their respective antioxidant (Catalase = DHE oxidation attributable to hydrogen peroxide, SOD = DHE oxidation attributable to superoxide, SOD/Catalase = DHE oxidation attributable to both superoxide and hydrogen peroxide). The MFI average of triplicate sets of cells incubated with DHE + SOD or catalase was subtracted from the MFI average of cells incubated with DHE alone. All values are normalized to control cells incubated with polyethylene glycol-SOD. Statistical significance based on Student's *t*-test (*$p < 0.04$). **(D)** MitoSOX oxidation determined in DC and normal control cells at P8 with FACS analysis. Values are relative to controls and error bars indicate standard deviation of triplicate sets of MFI determined on cohorts of 10,000 cells. Statistical significance based on Student's *t*-test (*$p < 0.01$). **(E)** Freshly acquired and positively selected $CD3^+$ T-cells from a subset of patients (DC-4 and DC-5) were subjected to DHE-FACS analysis. Error bars indicate standard deviation of triplicate sets. Both DC samples exhibited significant increase in DHE compared to age-matched controls (Student's *t*-test; *$p < 0.05$; **$p < 0.001$) (T-cells: Age-matched Control-1 *vs*. DC-5; Age-matched Control-2 *vs*. DC-4). **(F)** Early passage (P3) skin DC-1 skin keratinocytes and normal control keratinocytes at the same passage were assessed for DHE by FACS. Error bars indicate standard deviation of triplicate sets. **Statistically significant increase compared to normal cells (Student's *t*-test, $p < 0.001$).

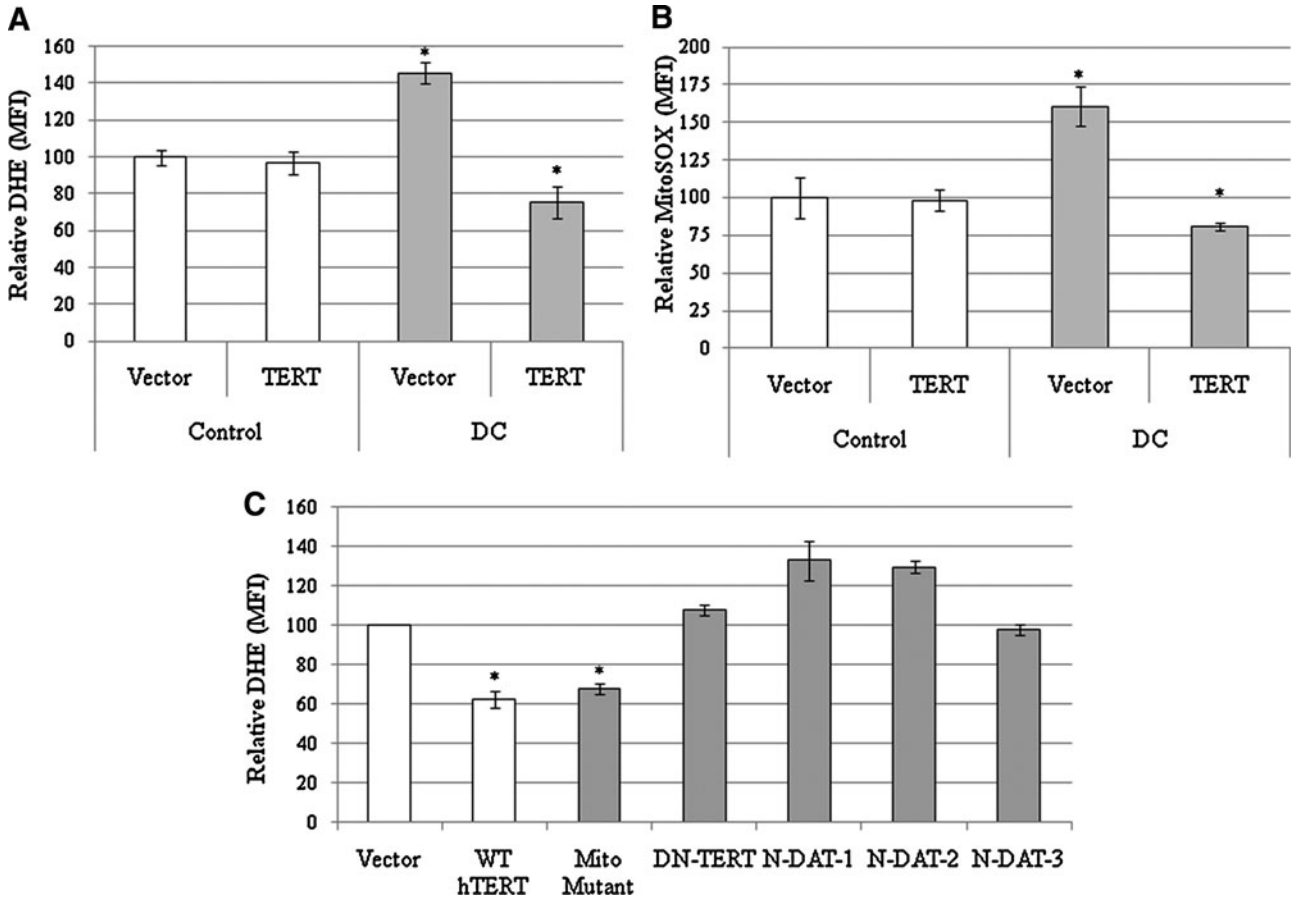

FIG. 4. Decreased levels of DHE oxidation seen in DC cells overexpressing TERT. (A, B) DC-1 fibroblasts were infected with retroviral vector alone or with a TERT expressing vector and selected for a pure population. These cells were then subjected to DHE-FACS **(A)** or MitoSOX-FACS **(B)** analysis. Error bars indicate standard deviation of triplicate sets. *Significant increase in DC cells compared to normal controls or significant decrease in DC-TERT expressing cells compared to the empty vector DC-1 control (Student's *t*-test, $p < 0.005$). Cells were normalized to empty vector controls. **(C)** DC-1 cells were stably infected with the indicated retroviral vector, selected *via* antibiotic resistance, and analyzed using the DHE-FACS assay. DHE oxidation values are relative to an empty vector control. Mito-Mutant (R3E/R6E), dominant-negative TERT, and N-dissociation of activities of telomerase (DAT) mutants 1–3 have been reported elsewhere. Error bars indicate standard deviation of triplicate sets of 10,000 cell cohorts analyzed individually. *Statistical significance decrease in DHE compared to controls, $p < 0.001$.

that has previously been demonstrated to disrupt telomeres (29) was overexpressed in normal fibroblasts. Expression of DN-TRF2 caused a significant 38% increase in DHE oxidation relative to vector control ($p < 0.005$; Supplementary Fig. S7), demonstrating that inducing telomere dysfunction in non-DC cells could also lead to increased steady-state levels of superoxide.

Suppression of increased steady-state levels of superoxide in DC cells by decreasing expression of p53 or p21$^{WAF/CIP}$

To determine whether expression of p53 and p21$^{WAF/CIP}$ was causally related to the increased steady-state levels of superoxide seen in DC cells, cells were infected with retroviral vectors expressing shRNA sequences targeting p53 or p21$^{WAF/CIP}$, selected with appropriate antibiotics, and then evaluated for DHE oxidation. Stable knockdown of p53 or p21$^{WAF/CIP}$ transcripts caused significant reduction in p53 and p21$^{WAF/CIP}$ transcripts (Supplementary Fig. S5) and a significant reduction in DHE oxidation (Fig. 5A), and this suppression of steady-state levels of superoxide was maintained with further passaging (data not shown). In contrast, experiments performed in parallel, knocking down p16^{INK4A}, failed to decrease ROS during cell passage, suggesting a specific role for p53/p21$^{WAF/CIP}$ in regulating superoxide levels in DC cells (data not shown). Continued passaging of cells with knocked down p53 or p21$^{WAF/CIP}$ uncovered an extension of proliferative lifespan with increased proliferation being more pronounced in the p53 knockdown cells (Fig. 5B). These results indicate that the downstream mediator of p53, p21$^{WAF/CIP}$, is essential for the increased levels of superoxide in DC cells, but that it is not the sole mediator of p53-associated inhibition of proliferation.

DC fibroblasts decrease mitochondrially derived superoxide and acquire improved growth kinetics when cultured in reduced O_2 without altering DDR

Cell culture is routinely performed under atmospheric oxygen tension (*i.e.*, 21%). *In vivo*, however, most cells are exposed to significantly less oxygen. Previous research has

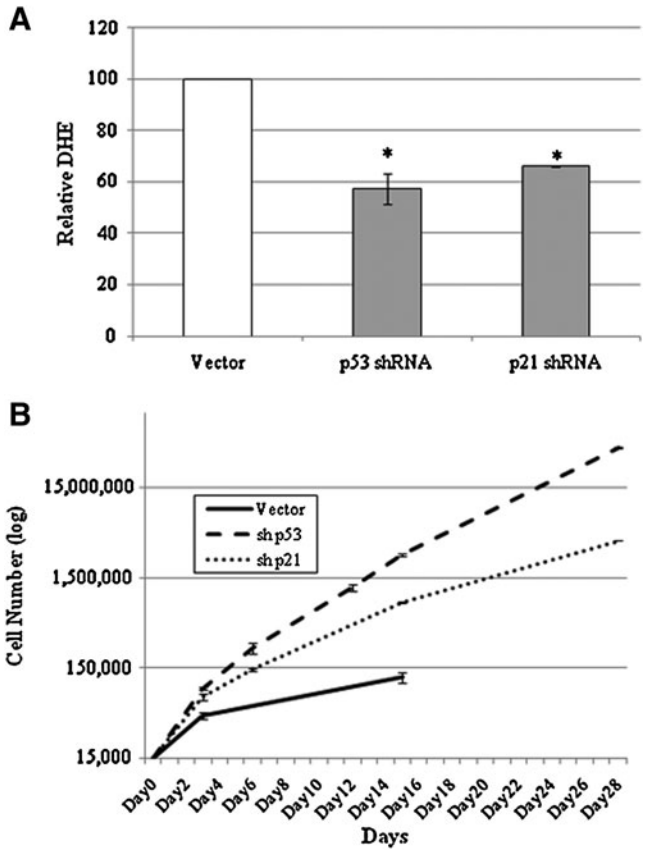

FIG. 5. Consequence of p53 or p21$^{WAF/CIP}$ shRNA expression on DHE oxidation, and proliferation in DC cells. (A) Passage 4 DC-1 cells were stably infected with shRNA knocking down the expression of p53 and p21. Cells were analyzed using DHE-FACS analysis at regular intervals to assess DHE staining and late passage (P10) vector cells and their shRNA counterparts are presented here. Vector controls and shRNA cells were performed in parallel (triplicate) to evaluate relative DHE oxidation. Values are relative to an empty vector control analyzed with the cells of interest. Error bars indicated standard deviation of triplicate sets. Symbol indicates statistically significant decrease in DHE oxidation compared to controls: $^*p < 0.001$. **(B)** Passage 8 DC-1 fibroblasts expressing a vector control, p53 shRNA, or p21 shRNA were plated at equivalent cell numbers and passaged in subconfluent conditions until senescence. Triplicate plates of cells were counted using a Coulter counter.

revealed that skin fibroblasts are afforded an extension of lifespan when grown in low oxygen (~4% *vs*. 21% atmospheric O_2) and conversely demonstrate diminished lifespan at levels greater than atmospheric O_2 (17). To determine the biological effects of manipulating O_2 tension, mid-passage (*i.e.*, passage 8) DC and control fibroblasts were grown in subconfluent conditions under atmospheric (21%) or low O_2 (4%) and passaged over a period of 14 days. DC cells demonstrated prolonged growth kinetics compared to control cells grown under ambient O_2 as previously described (Fig. 6A: population doubling time: 2.4 days *vs*. 1.7 days, respectively; solid gray *vs*. solid black lines) (50). Control cells grown in 4% O_2 displayed similar growth kinetics compared to those grown in ambient O_2 (population doubling time: 1.7 days *vs*. 1.7 days; black lines). In contrast to normal cells, DC cells cultured in low O_2 acquired significantly improved growth kinetics compared to ambient O_2 (Fig. 6A: population doubling time: 2.4 days for ambient *vs*. 1.9 days for low O_2; gray lines). At the termination of this 14-day proliferation experiment, DC cells demonstrated a twofold increase in cell number grown in low O_2 compared to DC cells grown in atmospheric O_2 tension. Interestingly, no significant changes in 53BP1 foci were found in DC cells grown in ambient O_2 *versus* low O_2, indicating that alterations in the DNA damage response was not contributing to the improved proliferative response seen in the DC cells in low O_2 (Fig. 6B). In addition, p21$^{WAF/CIP}$ levels were found to remain stable between cells grown in 4% O_2 and those grown in ambient O_2 in DC cells but were slightly decreased in normal cells, suggesting that growth in low O_2 caused a dissociation between DDR and inhibition of proliferative potential (Fig. 6C). This is in contrast to TERT-expressing DC cells in which levels of p21$^{WAF/CIP}$ were found to also be decreased (Fig. 6C). In addition, TERT expression in normal cells did not cause a significant decrease in p21$^{WAF/CIP}$ levels, suggesting that the steady-state levels of p21$^{WAF/CIP}$ protein in normal cells was not due to telomere dysfunction.

To determine if DC cells grown in 4% O_2 demonstrated alterations in steady-state levels of mitochondrial superoxide, MitoSOX oxidation was determined under the different O_2 tensions. Interestingly, MitoSOX oxidation was significantly reduced in 4% O_2 but only for DC cells and not normal cells (Fig. 6D). These results indicate that low O_2 conditions specifically improved DC growth kinetics as well as decreasing steady-state levels of mitochondrial derived superoxide in the absence of causing changes in the DNA damage response or expression of p21$^{WAF/CIP}$.

Discussion

Cells derived from DC patients with telomerase mutations afford a unique opportunity to isolate the effects of telomerase dysfunction and telomere shortening in otherwise young cells that have not been extensively passaged in culture. DC cells have prematurely shortened telomeres as well as characteristics of cellular aging, which include increased β-Gal staining, a large cytoplasmic-to-nuclear ratio, increased population doubling time, and decreased lifespan in culture. Given that DC patients display a unique clinical phenotype and acquire symptoms of premature aging, we set out to further characterize the molecular mechanisms, whereby telomere dysfunction engages cellular aging. Our studies confirm and extend previous results and, importantly, validate these findings in a relevant human disease caused by telomerase dysfunction.

The DDR related to telomere attrition has been well characterized in previous reports in senescent cells or cells undergoing telomere dysfunction (14). The increase in 53BP1 foci seen in DC cells (Fig. 1) extends and confirms these findings in the DC model system. Likewise, the current finding that p53/p21$^{WAF/CIP}$ is responsive to telomere dysfunction also confirms in the DC model system findings that were anticipated based on results in other model systems (24). Several studies indicate that activation of p53 and p21$^{WAF/CIP}$ in the context of telomerase or telomere dysfunction are not equivalent. For example, crossing p21$^{WAF/CIP}$ knockout mice into a telomerase negative background partially rescued the aging phenotype seen in later-generation telomerase knockout mice

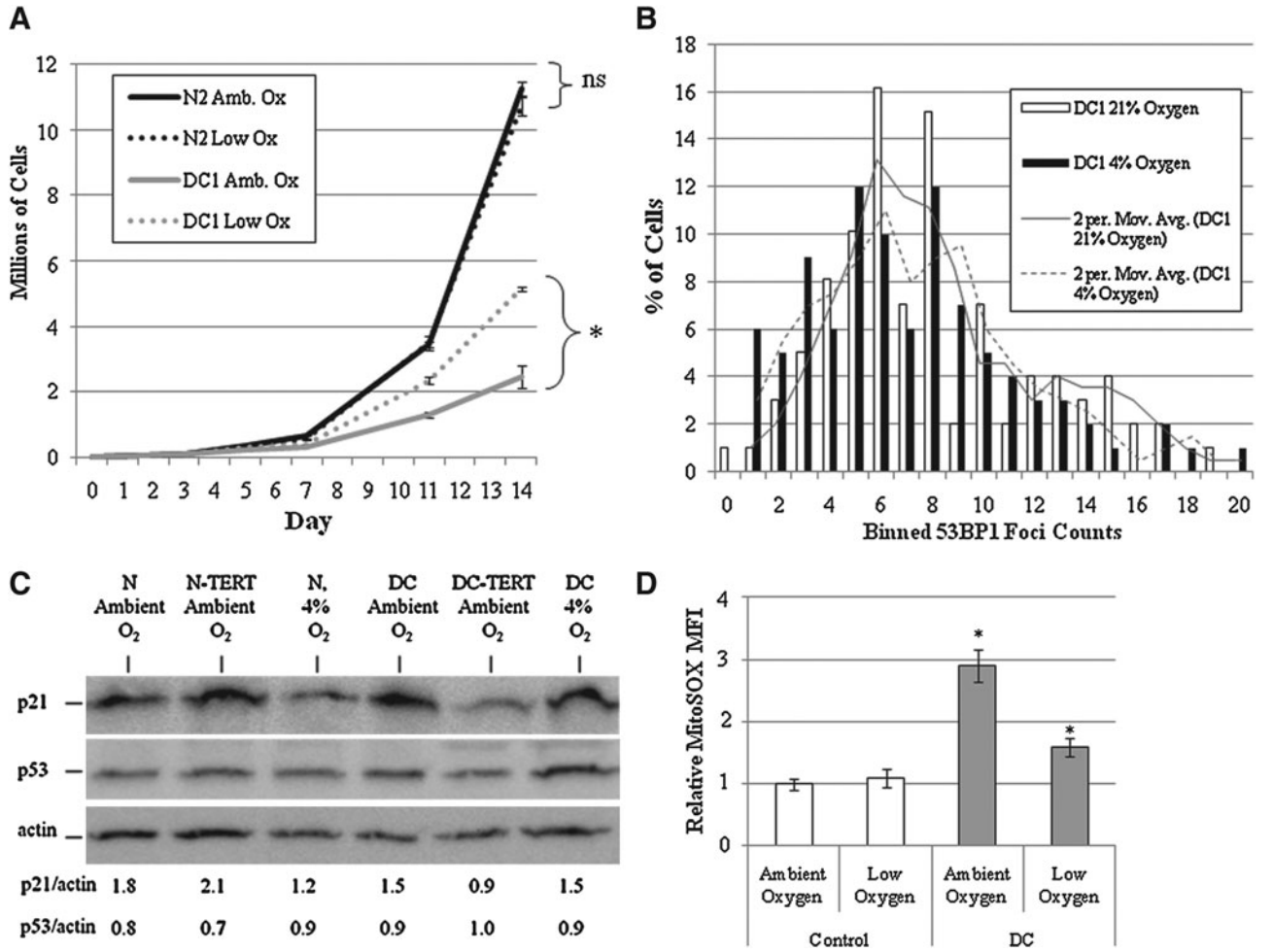

FIG. 6. Reducing O_2 tension suppresses inhibition of proliferative potential in DC fibroblasts. (A) DC-1 and control normal fibroblasts at passage 8 were grown at either ambient O_2 (21%) or low O_2 (4%) over a 2-week period. Triplicate sets of plates were passed at ~50%–70% confluency and quantified by a Coulter counter. Error bars represent the standard deviation of each triplicate set counted. *Significant difference (Student's *t*-test) in total cell counts at day 14: $p < 0.001$; ns indicates no statistically significant difference in cell counts. **(B)** DC-1 and control normal cells were grown in low and ambient oxygen for a week, fixed, and assessed with immunofluorescence to quantify 53BP1 foci. The foci of each nucleus were counted and binned accordingly. Comparisons were drawn using Student's *t*-test, indicating no statistical difference ($p < 0.25$). **(C)** $p21^{WAF/CIP}$ and p53 levels were evaluated by Western blotting in DC-1 and normal control cells grown under routine cell culture conditions (ambient O_2), transduced with TERT (also ambient O_2) as well as grown in low O_2 (4%). Levels of protein were quantified by evaluating band intensities *via* Fuji Multigauge densitometry software (version 2.3). These values were then normalized by dividing the quantified $p21^{WAF/CIP}$ band intensity by the intensity of their respective loading control (Actin). **(D)** DC-1 and control normal cells were grown in low and ambient O_2 for 1 week and then incubated in MitoSOX and subjected to FACS analysis. The data generated were subjected to the Student's *t*-test for significance. Significance was found when analyzing control cells grown in ambient O_2 *versus* DC cells grown in ambient as well as DC cells grown in ambient *versus* DC cells grown in low O_2 ($p < 0.005$ for both).

without increasing risk for tumorigenesis (11). This is in contrast to double knockouts of p53 and telomerase in which frequency of malignancy is dramatically increased (10). A more recent study using conditional knockout mice demonstrated that absence of p53 in the context of telomere dysfunction causes a high level of genetic instability and increased apoptosis as compared to $p21^{WAF/CIP}$ knockout mice (6). Our studies with cells from DC patients showed that knocking down p53 or $p21^{WAF/CIP}$ using shRNA resulted in an increase in lifespan and maintenance of proliferative capacity, but the effect on proliferation was more pronounced with knockdown of p53. Interestingly, DC cells expressing $p21^{WAF/CIP}$ shRNA had fewer telomere fusions and chromosome abnormalities than DC cells expressing p53 shRNA (unpublished observations), thus supporting the mouse studies. Both cell types did eventually undergo cessation of growth, most likely because telomeres became too short to support cell division. These results suggest that inhibition of $p21^{WAF/CIP}$ in the context of telomerase insufficiency might safely extend proliferative lifespan, but not indefinitely.

Previous studies have implicated p53 and $p21^{WAF/CIP}$ in modulating ROS levels (25, 27, 36). For example, enforced expression of p53 or $p21^{WAF/CIP}$ has been shown to cause increases in ROS (25, 36). In one study, the authors found that when p53 was intact, cancer cells expressing exogenous $p21^{WAF/CIP}$ would become apoptotic, whereas cells that had

lost or inactivated p53 underwent senescence (25). Both these biological outcomes could be inhibited by the thiol antioxidant *N*-acetyl cysteine (NAC), supporting the conclusion that oxidative stress was involved in the mechanism growth inhibition. In another study, the authors found that enforced expression of $p21^{WAF/CIP}$ increased ROS and β-Gal staining and this was suppressed by NAC in cancer cells, again supporting the conclusion that ROS caused entry into senescence (36). Interestingly, we were unable to extend the lifespan or increase proliferative capacity of DC cells by NAC treatment (data not shown), most likely because of well-documented cell cycle inhibition properties of NAC on primary fibroblasts (38). Our observations showing improved proliferation and lower levels of MitoSOX fluorescence in DC cells when grown in 4% oxygen conditions indicates a redox-mediated component of senescence in DC cells. Increased ROS in DC cells could be necessary to maintain cells in senescence or it could be involved in causing more cellular damage and accelerating senescence in a positive feedback loop as has been speculated previously (39, 40). Further studies will be needed to clarify these issues.

The mechanism by which the $p53/p21^{WAF/CIP}$ pathway, in the context of telomerase/telomere dysfunction, leads to increases in steady-state levels of superoxide is not entirely clear. A previous study found that cells from telomerase knockout mice with short telomeres had decreased CAT expression (which is expected to lead to increased steady-state levels of hydrogen peroxide) as well as increased TGF-β1 and Collagen IV (41). However, the role of the $p53/p21^{WAF/CIP}$ pathway was not examined in that study. Interestingly, we did not observe changes in levels of mRNA expression of catalase or superoxide dismutates in DC cells as compared to normal cells (data not shown). In another study by Lee *et al.*, T-oligos were utilized to mimic telomere dysfunction (35), and this was found to activate p53 causing an apparent increase in NADPH oxidase-dependent ROS levels based on the finding that ROS levels could be attenuated by treatment with a nonspecific inhibitor of flavin containing oxidases (diphenyliodonium). A recent study utilized what was referred to as *in silico* interactome analysis to generate a model implicating dysfunctional telomeres (caused by overexpression of a dominant negative version of the telomere binding protein TRF2) in the activation of $p53/p21^{WAF/CIP}$, followed by induction of mitochondrial dysfunction and production of ROS in the mitochondria through serial signaling by the effectors GADD45-MAPK14-GRB2-TGFBR2-TGF-beta (40). This latter study suggests a complex pathway to explain how dysfunctional telomeres lead to increased ROS. Although our results do not clearly identify the source of increased steady-state levels of superoxide in the DC cells, our findings showing MitoSOX oxidation being altered, coupled with the differential effects seen with manipulations of O_2 tension, support the hypothesis that mitochondria may represent a significant source of superoxide in DC cells containing dysfunctional telomerase and telomeres. This is of interest because recent studies have implicated TERT in localizing to the mitochondria and modulating ROS (1, 42, 43). However, our studies showing that a TERT mutant without a mitochondria localization signal was still able to reduce steady-state levels of superoxide in DC cells do not support this model. Further studies will be needed to clarify precisely how telomerase dysfunction and short telomeres increase ROS and how the mitochondria are involved in this process.

The findings of this current work support the hypothesis that oxidative stress may have a previously unappreciated function in the constellation of symptoms and pathologies found in DC patients. Given previous reports in other disease pathologies, it is logical to hypothesize that oxidative stress may contribute to bone marrow failure and pulmonary fibrosis seen in DC patients. Bone marrow failure has been attributed to the failure of the hematopoietic stem cell niche and stroma to support the most immature bone marrow cells and this niche may be especially susceptible to dysfunctional telomeres associated with increased steady-state levels of superoxide (28). The oxidative stress mechanism is also likely to contribute to pulmonary fibrosis, as ROS-mediated signaling has been hypothesized to contribute to cell damage and profibrogenic stimuli in many other disease states involving fibrosis (31). Given the widespread investigation of antioxidant therapies to mitigate these types of tissue injury processes, it is possible that DC patients could benefit from adjuvant antioxidant therapies that could represent relatively noninvasive and potentially effective strategies for this as yet incurable disease.

In conclusion, the current study supports the hypothesis that insufficient telomerase activity and concomitant telomere attrition activate a DNA damage response that is accompanied by increased steady-state levels of superoxide in a $p53/p21^{WAF/CIP}$-dependent fashion in cells from DC patients. This represents a significant finding because it suggests in a very relevant human model of aging that telomere dysfunction and oxidative stress may not be mutually exclusive mechanisms promoting organismal aging but may represent an integrated process amenable to both genetic as well as pharmacological manipulation.

Acknowledgments

Retroviral constructs were kindly provided by different laboratories and individuals. These include sh-p53 pBABE-hygro (Dr. Carla Grandori), sh-p21-GIPZ (Dr. Toru Nyunoya), sh-p16 MSCV (Dr. Scott Lowe), dominant-negative TERT-pBABE-neo (Dr. Bill Hahn), TERT-DAT mutants (N-DAT +92, +122, +128) in pBABE-neo (Dr. Christopher Counter), DN-TRF2-pBABE-Puro (Titia de Lange), and TERT-pBABE-neo (Dr. Robert Weinberg). We thank Francoise Gourronc for help with QRT-PCR. We acknowledge the University of Iowa Microscopy Core, DNA Core, Gene Vector Core, Flow Cytometry Core, and Radiation and Free Radical Research Core in the Holden Comprehensive Cancer Center for performing assays and providing equipment and guidance for this research. This work was supported by NIH RO1 AG027388 (AJK), NIH P30 DK54759 (Vector Core), NIH P30 CA086862 (DRS), and DOE DE-SC0000830 (DRS and NAB). ERW was partly supported by a grant from the American Heart Association (0910133G) and the University of Iowa Program in Genetics Predoctoral Training Grant (T32 GM08629).

Author Disclosure Statement

No competing financial interests exist.

References

1. Ahmed S, Passos JF, Birket MJ, Beckmann T, Brings S, Peters H, Birch-Machin MA, von Zglinicki T, and Saretzki G.

Telomerase does not counteract telomere shortening but protects mitochondrial function under oxidative stress. *J Cell Sci* 121: 1046–1053, 2008.
2. Anderson ME. *Handbook of Methods for Oxygen Radical Research*. Boca Raton, FL: CRC Press, Inc., 1985.
3. Armbruster BN, Banik SS, Guo C, Smith AC, and Counter CM. N-terminal domains of the human telomerase catalytic subunit required for enzyme activity *in vivo*. *Mol Cell Biol* 21: 7775–7786, 2001.
4. Aubert G and Lansdorp PM. Telomeres and aging. *Physiol Rev* 88: 557–579, 2008.
5. Aykin-Burns N, Ahmad IM, Zhu Y, Oberley L, and Spitz DR. Increased levels of superoxide and hydrogen peroxide mediate the differential susceptibility of cancer cells vs. normal cells to glucose deprivation. *Biochem J* 418: 29–37, 2009.
6. Begus-Nahrmann Y, Lechel A, Obenauf AC, Nalapareddy K, Peit E, Hoffmann E, Schlaudraff F, Liss B, Schirmacher P, Kestler H, Danenberg E, Barker N, Clevers H, Speicher MR, and Rudolph KL. p53 deletion impairs clearance of chromosomal-instable stem cells in aging telomere-dysfunctional mice. *Nat Genet* 41: 1138–1143, 2009.
7. Bodnar AG, Ouellette M, Frolkis M, Holt SE, Chiu CP, Morin GB, Harley CB, Shay JW, Lichtsteiner S, and Wright WE. Extension of life-span by introduction of telomerase into normal human cells. *Science* 279: 349–352, 1998.
8. Bollmann FM. The many faces of telomerase: emerging extratelomeric effects. *Bioessays* 30: 728–732, 2008.
9. Boveris A and Chance B. The mitochondrial generation of hydrogen peroxide. General properties and effect of hyperbaric oxygen. *Biochem J* 134: 707–716, 1973.
10. Chin L, Artandi SE, Shen Q, Tam A, Lee SL, Gottlieb GJ, Greider CW, and DePinho RA. p53 deficiency rescues the adverse effects of telomere loss and cooperates with telomere dysfunction to accelerate carcinogenesis. *Cell* 97: 527–538, 1999.
11. Choudhury AR, Ju Z, Djojosubroto MW, Schienke A, Lechel A, Schaetzlein S, Jiang H, Stepczynska A, Wang C, Buer J, Lee HW, von Zglinicki T, Ganser A, Schirmacher P, Nakauchi H, and Rudolph KL. Cdkn1a deletion improves stem cell function and lifespan of mice with dysfunctional telomeres without accelerating cancer formation. *Nat Genet* 39: 99–105, 2007.
12. Collins K and Mitchell JR. Telomerase in the human organism. *Oncogene* 21: 564–579, 2002.
13. Cong YS, Wright WE, and Shay JW. Human telomerase and its regulation. *Microbiol Mol Biol Rev* 66: 407–425, table of contents, 2002.
14. d'Adda di Fagagna F, Reaper PM, Clay-Farrace L, Fiegler H, Carr P, Von Zglinicki T, Saretzki G, Carter NP, and Jackson SP. A DNA damage checkpoint response in telomere-initiated senescence. *Nature* 426: 194–198, 2003.
15. Darbro BW, Lee KM, Nguyen NK, Domann FE, and Klingelhutz AJ. Methylation of the p16(INK4a) promoter region in telomerase immortalized human keratinocytes co-cultured with feeder cells. *Oncogene* 25: 7421–7433, 2006.
16. Dimri GP, Lee X, Basile G, Acosta M, Scott G, Roskelley C, Medrano EE, Linskens M, Rubelj I, Pereira-Smith O, *et al.* A biomarker that identifies senescent human cells in culture and in aging skin *in vivo*. *Proc Natl Acad Sci U S A* 92: 9363–9367, 1995.
17. Finkel T and Holbrook NJ. Oxidants, oxidative stress and the biology of ageing. *Nature* 408: 239–247, 2000.
18. Golubev AG. [The other side of metabolism]. *Biokhimiia* 61: 2018–2039, 1996.
19. Gourronc FA, Robertson MM, Herrig AK, Lansdorp PM, Goldman FD, and Klingelhutz AJ. Proliferative defects in dyskeratosis congenita skin keratinocytes are corrected by expression of the telomerase reverse transcriptase, TERT, or by activation of endogenous telomerase through expression of papillomavirus E6/E7 or the telomerase RNA component, TERC. *Exp Dermatol* 19: 279–288, 2010.
20. Griffith JD, Comeau L, Rosenfield S, Stansel RM, Bianchi A, Moss H, and de Lange T. Mammalian telomeres end in a large duplex loop. *Cell* 97: 503–514, 1999.
21. Griffith OW. Determination of glutathione and glutathione disulfide using glutathione reductase and 2-vinylpyridine. *Anal Biochem* 106: 207–212, 1980.
22. Hahn WC, Stewart SA, Brooks MW, York SG, Eaton E, Kurachi A, Beijersbergen RL, Knoll JH, Meyerson M, and Weinberg RA. Inhibition of telomerase limits the growth of human cancer cells. *Nat Med* 5: 1164–1170, 1999.
23. Harley CB. Telomere loss: mitotic clock or genetic time bomb? *Mutat Res* 256: 271–282, 1991.
24. Herbig U, Jobling WA, Chen BP, Chen DJ, and Sedivy JM. Telomere shortening triggers senescence of human cells through a pathway involving ATM, p53, and p21(CIP1), but not p16(INK4a). *Mol Cell* 14: 501–513, 2004.
25. Inoue T, Kato K, Kato H, Asanoma K, Kuboyama A, Ueoka Y, Yamaguchi S, Ohgami T, and Wake N. Level of reactive oxygen species induced by p21Waf1/CIP1 is critical for the determination of cell fate. *Cancer Sci* 100: 1275–1283, 2009.
26. Jacobs JJ and de Lange T. Significant role for p16INK4a in p53-independent telomere-directed senescence. *Curr Biol* 14: 2302–2308, 2004.
27. Johnson TM, Yu ZX, Ferrans VJ, Lowenstein RA, and Finkel T. Reactive oxygen species are downstream mediators of p53-dependent apoptosis. *Proc Natl Acad Sci U S A* 93: 11848–11852, 1996.
28. Ju Z, Jiang H, Jaworski M, Rathinam C, Gompf A, Klein C, Trumpp A, and Rudolph KL. Telomere dysfunction induces environmental alterations limiting hematopoietic stem cell function and engraftment. *Nat Med* 13: 742–747, 2007.
29. Karlseder J, Broccoli D, Dai Y, Hardy S, and de Lange T. p53- and ATM-dependent apoptosis induced by telomeres lacking TRF2. *Science* 283: 1321–1325, 1999.
30. Kim NW, Piatyszek MA, Prowse KR, Harley CB, West MD, Ho PL, Coviello GM, Wright WE, Weinrich SL, and Shay JW. Specific association of human telomerase activity with immortal cells and cancer. *Science* 266: 2011–2015, 1994.
31. Kinnula VL, Fattman CL, Tan RJ, and Oury TD. Oxidative stress in pulmonary fibrosis: a possible role for redox modulatory therapy. *Am J Respir Crit Care Med* 172: 417–422, 2005.
32. Kirwan M and Dokal I. Dyskeratosis congenita: a genetic disorder of many faces. *Clin Genet* 73: 103–112, 2008.
33. Knudson M, Kulkarni S, Ballas ZK, Bessler M, and Goldman F. Association of immune abnormalities with telomere shortening in autosomal-dominant dyskeratosis congenita. *Blood* 105: 682–688, 2005.
34. Ku HH, Brunk UT, and Sohal RS. Relationship between mitochondrial superoxide and hydrogen peroxide production and longevity of mammalian species. *Free Radic Biol Med* 15: 621–627, 1993.
35. Lee MS, Yaar M, Eller MS, Runger TM, Gao Y, and Gilchrest BA. Telomeric DNA induces p53-dependent reactive oxygen species and protects against oxidative damage. *J Dermatol Sci* 56: 154–162, 2009.

36. Macip S, Igarashi M, Fang L, Chen A, Pan ZQ, Lee SW, and Aaronson SA. Inhibition of p21-mediated ROS accumulation can rescue p21-induced senescence. *EMBO J* 21: 2180–2188, 2002.
37. Masutomi K, Possemato R, Wong JM, Currier JL, Tothova Z, Manola JB, Ganesan S, Lansdorp PM, Collins K, and Hahn WC. The telomerase reverse transcriptase regulates chromatin state and DNA damage responses. *Proc Natl Acad Sci U S A* 102: 8222–8227, 2005.
38. Menon SG, Sarsour EH, Kalen AL, Venkataraman S, Hitchler MJ, Domann FE, Oberley LW, and Goswami PC. Superoxide signaling mediates *N*-acetyl-L-cysteine-induced G1 arrest: regulatory role of cyclin D1 and manganese superoxide dismutase. *Cancer Res* 67: 6392–6399, 2007.
39. Muller M. Cellular senescence: molecular mechanisms, *in vivo* significance, and redox considerations. *Antioxid Redox Signal* 11: 59–98, 2009.
40. Passos JF, Nelson G, Wang C, Richter T, Simillion C, Proctor CJ, Miwa S, Olijslagers S, Hallinan J, Wipat A, Saretzki G, Rudolph KL, Kirkwood TB, and von Zglinicki T. Feedback between p21 and reactive oxygen production is necessary for cell senescence. *Mol Syst Biol* 6: 347, 2010.
41. Perez-Rivero G, Ruiz-Torres MP, Diez-Marques ML, Canela A, Lopez-Novoa JM, Rodriguez-Puyol M, Blasco MA, and Rodriguez-Puyol D. Telomerase deficiency promotes oxidative stress by reducing catalase activity. *Free Radic Biol Med* 45: 1243–1251, 2008.
42. Santos JH, Meyer JN, Skorvaga M, Annab LA, and Van Houten B. Mitochondrial hTERT exacerbates free-radical-mediated mtDNA damage. *Aging Cell* 3: 399–411, 2004.
43. Santos JH, Meyer JN, and Van Houten B. Mitochondrial localization of telomerase as a determinant for hydrogen peroxide-induced mitochondrial DNA damage and apoptosis. *Hum Mol Genet* 15: 1757–1768, 2006.
44. Shieh SY, Ikeda M, Taya Y, and Prives C. DNA damage-induced phosphorylation of p53 alleviates inhibition by MDM2. *Cell* 91: 325–334, 1997.
45. Simons AL, Ahmad IM, Mattson DM, Dornfeld KJ, and Spitz DR. 2-Deoxy-D-glucose combined with cisplatin enhances cytotoxicity via metabolic oxidative stress in human head and neck cancer cells. *Cancer Res* 67: 3364–3370, 2007.
46. Slane BG, Aykin-Burns N, Smith BJ, Kalen AL, Goswami PC, Domann FE, and Spitz DR. Mutation of succinate dehydrogenase subunit C results in increased O2.-, oxidative stress, and genomic instability. *Cancer Res* 66: 7615–7620, 2006.
47. Takahashi A, Ohtani N, Yamakoshi K, Iida S, Tahara H, Nakayama K, Nakayama KI, Ide T, Saya H, and Hara E. Mitogenic signalling and the p16INK4a-Rb pathway cooperate to enforce irreversible cellular senescence. *Nat Cell Biol* 8: 1291–1297, 2006.
48. von Zglinicki T, Saretzki G, Docke W, and Lotze C. Mild hyperoxia shortens telomeres and inhibits proliferation of fibroblasts: a model for senescence? *Exp Cell Res* 220: 186–193, 1995.
49. Vulliamy T, Marrone A, Goldman F, Dearlove A, Bessler M, Mason PJ, and Dokal I. The RNA component of telomerase is mutated in autosomal dominant dyskeratosis congenita. *Nature* 413: 432–435, 2001.
50. Westin ER, Chavez E, Lee KM, Gourronc FA, Riley S, Lansdorp PM, Goldman FD, and Klingelhutz AJ. Telomere restoration and extension of proliferative lifespan in dyskeratosis congenita fibroblasts. *Aging Cell* 6: 383–94, 2007.

Address correspondence to:
Dr. Aloysius J. Klingelhutz
Department of Microbiology
University of Iowa
2202 MERF, 375 Newton Road
Iowa City, IA 52242

E-mail: aloysius-klingelhutz@uiowa.edu

Date of first submission to ARS Central, July 1, 2010; date of final revised submission, November 17, 2010; date of acceptance, November 17, 2010.

Abbreviations Used

53BP1 = p53 binding protein 1
ADDC = autosomal dominant dyskeratosis congenita
DAT = dissociation of activities of telomerase
DDR = DNA Damage Response
DHE = dihydroethidium
GSH = glutathione
GSSG = glutathione disulfide
NAC = *N*-acetylcysteine
$p16^{INK4A}$ = protein 16 inhibitor of kinase 4a
$p21^{WAF/CIP}$ = protein 21 wild-type p53 activation factor/Cdk-interacting protein
PEG = polyethylene glycol
QRT-PCR = quantitative reverse transcriptase–polymerase chain reaction
ROS = reactive oxygen species
shRNA = short-hairpin RNA
SOD = superoxide dismutase
TERC = telomerase RNA component
TERT = telomerase reverse transcriptase
TRF2 = telomere repeat binding factor 2